Bulletin of the Seismological Society of America, Vol. 100, No. 2, pp. 851–858, April 2010, doi: 10.1785/0120090057

Short Note

Lg Attenuation in a Region with Both Continental and Oceanic Environments

by Tae-Kyung Hong

Abstract The crustally-guided shear wave, *Lg*, is typically the strongest phase at regional distances. *Lg* phases are analyzed often for estimation of magnitudes of regional events. The variation of *Lg* in regions with both continental and oceanic environments has been rarely investigated. We investigate *Lg* attenuation in a plate-margin area around Korea and Japan that is encompassed by seas and oceans. The mean quality factor of *Lg* at 1 Hz (Q_0) is 498. The geometrical-spreading exponent term is estimated as 0.75. These observations characterize the study region as a high attenuation region compared to typical intraplate continental regions. Low-Q regions are widely developed over the Japanese islands, with some spotted high-Q regions. Relatively high Q is observed in most regions of the Korean Peninsula except a south-eastern part where a Cretaceous volcanic-sediment basin exists. The high-Q values are close to the typical Q value in continental crust. Significantly low Q of 100 or less is observed in most oceanic regions including the East Sea (Sea of Japan), the Pacific Ocean, and the South China Sea. The high attenuation of *Lg* in oceanic regions suggests possible underestimation of magnitudes of oceanic events. Thus, it appears that proper correction of *Lg* amplitude is highly desired for accurate estimation of magnitudes of regional oceanic events.

Introduction

The crustally-guided shear wave, *Lg*, is typically the strongest phase at regional distances, and its amplitude is rarely affected by the radiation pattern of source. Thus, *Lg* is widely used for estimation of the magnitudes of regional events. The *Lg* wave, however, is attenuated significantly in oceanic crust. Also, the *Lg* is highly influenced by lateral variation of crustal structure (e.g., Zhang and Lay, 1995; Kennett and Furumura, 2001).

The area around the Korean Peninsula, Japanese islands, and the East Sea (Sea of Japan) is a continental margin that abuts the Pacific Ocean. Complex tectonic activities in the region cause much seismic activity, not only inland but also in offshore regions around the East Sea and the subduction zones along the Japanese islands. The offshore events are normally well observed at regional stations in Korea and Japan. However, the offshore events are potential threats of tsunamis and seismic hazard to the onshore areas. Thus, accurate estimation of regional magnitudes are particularly important for offshore events.

A widely adopted regional magnitude scale is based on the *Lg* phase. Thus, it is highly desired to understand *Lg* attenuation for accurate estimation of magnitudes of regional oceanic events. Many studies on *Lg* attenuation have been made for various regions (e.g., Phillips *et al.*, 2000; Xie *et al.*, 2006; Chung *et al.*, 2007; Hong *et al.*, 2008). However, quantitative investigation of *Lg* attenuation along oceanic ray paths has been rarely made so far.

Dense seismic networks in the area of the Korean Peninsula and Japanese islands allowed us to investigate the *Lg* variation in a continental margin with back-arc region. We conducted a tomographic inversion of *Lg* quality factor (Q) in the region and inferred the tectonic implications from *LgQ* tomography. We also discuss the magnitude estimation from seismic records with oceanic ray paths.

Data and Geology

We collected seismic data from local and regional events in 2000–2008 with focal depths less than 35 km, which were recorded at stations in Korea, Japan, Taiwan, and China. The magnitudes of the events ranged between 2.7 and 7.9 (Fig. 1), where the magnitudes greater than 6 are based on the moment magnitude or surface-wave magnitude scales to avoid the saturation of body-wave magnitudes for large events (Lay and Wallace, 1995, p 383).

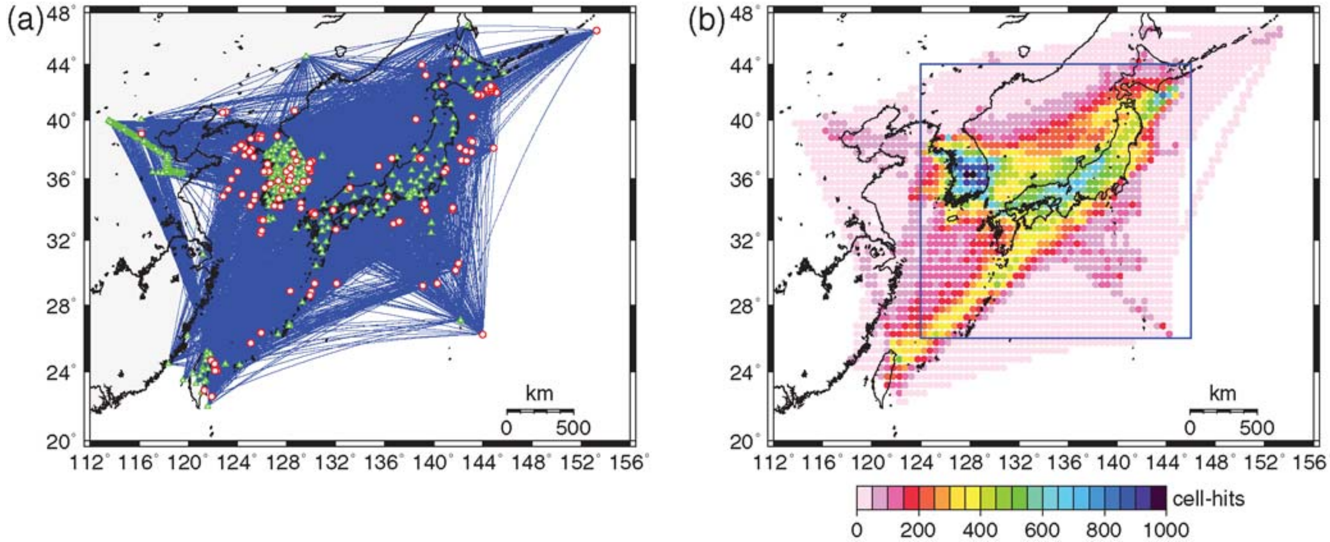

Figure 1. Maps for (a) locations of events, stations, and ray paths and (b) ray path density. The cell hits are counted in a domain discretized by 0.5°-by-0.5° cells. Circle, events; triangles, stations; solid lines, great-circle paths. The study area is denoted by a solid-line box in (b). The ray path coverage and density over the study area is good for a tomographic inversion.

The number of events was 141, and the number of stations was 446 (Figs. 1, 2). The total number of records collected was 15,492. The distribution of events and stations displays good ray-path coverage over the study area, particularly for the areas of South Korea, Japan, and the East Sea. The dense ray-path coverage allows a stable tomographic inversion. Event information was collected from event catalogues of local seismological institutions (Korea Institute of Geoscience and Mineral Resources [KIGAM], Korean Meteorological Administration [KMA]) and the International Seismological Centre (ISC). We analyzed records with epicentral distances less than 2500 km.

The crust of the East Sea has a transitional structure from continental to oceanic crusts, which accommodates undulated Moho topography as well as abrupt changes in crustal structure. *Lg* waves propagating across a thin crust suffer from high attenuation due to significant energy leakage into the mantle (Knopoff *et al.*, 1979; Kennett, 1986). In addition, *Lg* from a long ray path through an undulated crust displays energy diffusion beyond the typical group-velocity window (Zhang and Lay, 1995). The diffused wave train is possibly contaminated by other later phases (Campillo *et al.*, 1985). Thus, the transitional structure of the crust in the East Sea may cause high attenuation of *Lg*, which yields weak *Lg*.

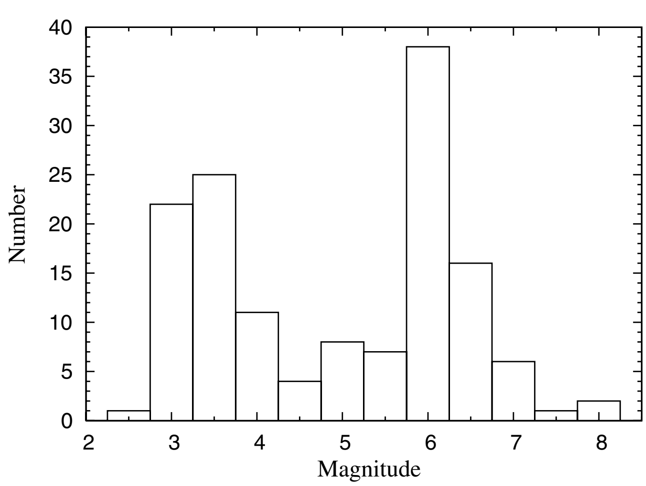

Figure 2. Histogram of event magnitudes. The total number of events was 141. The smallest magnitude was 2.7, and the largest magnitude was 7.9.

The maximum amplitude of *Lg*, however, develops in an early portion of the typical *Lg* wave train despite diffusion of *Lg* energy in an undulated crust, which allowed us to estimate the maximum *Lg* amplitude in the expected time window. Seismic records of four representative regional earthquakes with ray paths across the Korean Peninsula, Japanese islands, and the East Sea are presented in Figure 3. First arrivals of *P* and *S* phases (*Pn*, *Sn*) and the crustally guided shear waves (*Lg*) are marked on the figure. The *Lg* waves from continental ray paths are clearly observed, and those from ray paths crossing the East Sea are relatively weak but reasonably identifiable.

The far-east Asian region (northwestern Pacific) around the Korean Peninsula, the East Sea, and Japanese islands has experienced complex tectonic history. The Korean Peninsula was formed by the collision of massif blocks, which was completed during the Jurassic period (Chough *et al.*, 2000). Two fold belts intervene between the massif blocks. A volcanic-sedimentary basin developed in the southeastern Korean Peninsula during the Cretaceous period.

The East Sea was formed by a continental rifting during the Oligocene to mid-Miocene, which caused separation of the Japanese islands from the Eurasian Plate (Chough *et al.*, 2000). Three deep-seated back-arc basins (Japan, Yamato, and Ulleung basins) were developed during the opening. The opening of the East Sea was completed in the mid-Miocene period before its full development into an oceanic crust due to east–west directional shortening by the subduction of the Pacific Plate (Jolivet and Huchon, 1989). The crust of the East Sea thus shows a transitional structure between a continental crust and an oceanic crust (Kim *et al.*, 2003; Sato *et al.*, 2006).

The continental lithosphere of Japanese islands is significantly influenced by volcanic activity and tectonic compression, which are associated with subduction of the Pacific Plate and the Philippine Sea Plate. Many earthquakes occur along the subduction zones around the Japanese islands. Also, the current east–west directional tectonic compression causes shallow offshore seismicity in the East Sea.

Method

The spectral amplitude of *Lg* can be expressed as (Sereno *et al.*, 1988; Xie and Patton, 1999)

$$A_{ij}(f) = S_i(f)G(d_{ij})\exp\left[-\frac{\pi f d_{ij}}{v_g Q_{ij}(f)}\right]e_{ij}(f), \quad (1)$$

where $A_{ij}(f)$ is the *Lg* displacement ground motion at station j for event i and the frequency of f; $S_i(f)$ is the source spectrum of the event; $G(d_{ij})$ is the geometrical-spreading term at distance of d_{ij}; $Q_{ij}(f)$ is the quality factor along the ray path between event and station; v_g is the group velocity of *Lg*, which is given by 3500 m/sec; and $e_{ij}(f)$ is the cumulative effect of the other minor factors along the ray path.

The *Lg* quality factor, $Q_{ij}(f)$, can be expressed by

$$Q_{ij}(f) = Q_{0,ij} f^{\eta_{ij}}, \quad (2)$$

where $Q_{0,ij}$ is the quality factor at 1 Hz, and η_{ij} is the power-law frequency dependence term. The frequency-independent geometrical-spreading factor is given by (e.g., Hearn *et al.*, 2008)

$$G(d_{ij}) = (d_0/d_{ij})^{\gamma}, \quad (3)$$

where γ is the geometrical decay rate, and d_0 is a reference distance.

The source spectrum, $S_i(f)$, can be expressed as (Brune, 1970; Aki and Richards, 1980, p. 424)

$$S_i(f) = \frac{M_{0,i} R_{\theta\phi}}{4\pi\sqrt{\rho_s \rho_r v_s^5 v_r}(1 + f^2/f_{c,i}^2)}, \quad (4)$$

where $M_{0,i}$ is the seismic moment of event i, $f_{c,i}$ is the corner frequency, $R_{\theta\phi}$ is the amplitude scaling for radiation pattern, and ρ_r and v_r are the density and the *S*-wave velocity in the receiver region, respectively. *Lg* waves are crustally guided shear waves, which are multiply reflected in the crust. Thus, the *Lg* waves develop consistently, regardless of azimuth. We applied $R_{\theta\phi} = 0.60$ by taking into account the average radiation pattern of *S* waves (e.g., Fisk, 2007). Also, considering the crustal structure around the Korean Peninsula, we applied $v_r = 3273$ m/sec and $\rho_s = 2580$ kg/m^3 (Chang and Baag, 2005; Hong and Rhie, 2009).

We calculated the moments (M_0) and corner frequencies (f_c) of events using known source-parameter relationships with magnitude (Xie, 2002)

$$\begin{aligned} \log(M_0) &= 9.96 + 1.17M, \\ \log(f_c) &= 4.603 - 0.308\log(M_0), \end{aligned} \quad (5)$$

where M is the magnitude. From equations (4) and (5), we calculated the source spectrum $S(f)$ of each event. We deconvolved the source spectra from observed amplitudes to equalize the source influence. From equation (1), we have

$$\ln\left[\frac{A_{ij}(f)}{S_i(f)}\right] = -\gamma \ln d_{ij} - \frac{\pi f d_{ij}}{v_g Q_{ij}(f)} + C_{ij}(f), \quad (6)$$

where the geometrical-spreading exponent term, γ, is a frequency-independent constant, and C_i is a constant for influence from minor factors. We determine Q for a given frequency in a least-squares sense. It is noteworthy that the source parameters such as moment and corner frequency have linear relationships with respect to the magnitude as shown in equation (5). Under- or overestimation of source spectra can be made due to incorporation of inaccurate constant coefficients in the linear relationships that do not represent the source-spectral relationship in given area.

However, considering possible variations of the constant coefficients in the linear relationships, an inaccurate representation of source parameters based on the linear relationships causes either a constant level change or minimal variations of the logarithmic equalized amplitudes ($\ln[A_{ij}(f)/S_i(f)]$). Similarly, an implementation of different values of $R_{\theta\phi}$ can also cause a constant change in levels of equalized amplitudes. However, such constant level variation in the logarithmic equalized amplitudes does not cause any change in the estimates of γ and Q.

For a tomographic inversion, equation (6) is recast to be

$$\ln\left[\frac{A_{ij}(f)}{S_i(f)}\right] + \gamma \ln d_{ij} = a_i(f) + b_j(f) - \left[\frac{\pi f d_{ij}}{v_g}\right]\frac{1}{Q_{ij}(f)}, \quad (7)$$

where $a_i(f)$ and $b_j(f)$ are static amplitude–correction terms for event i and station j, respectively. Thus, equation (7) can be rewritten as

$$\mathbf{b} = \mathbf{A}\mathbf{x}, \quad (8)$$

where $\mathbf{b}$ is the vector for equalized amplitudes with correction for geometrical spreading, $\mathbf{A}$ is the kernel matrix, and $\mathbf{x}$ is the unknown vector to be determined, which is composed

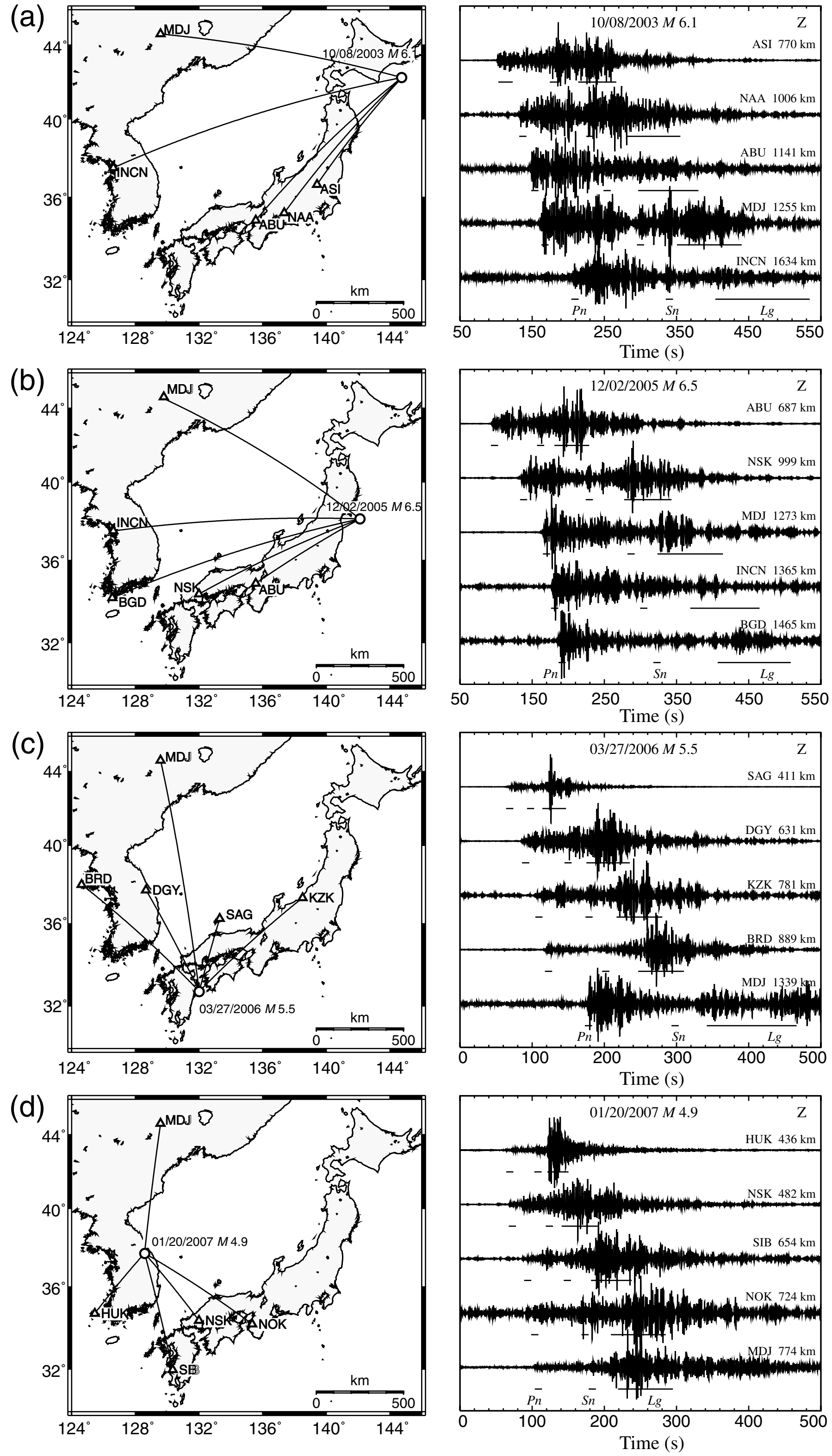

Figure 3. Vertical displacement seismograms for four regional earthquakes and their location maps: (a) M 6.1 earthquake on 8 October 2003; (b) M 6.5 earthquake on 2 December 2005; (c) M 5.5 earthquake on 27 March 2006; and (d) M 4.9 earthquake on 20 January 2007. Locations of events and stations are marked with open circles and triangles, respectively. The maps on the left column show the locations of events and stations along with the great-circle paths. Seismograms are band-pass filtered between 0.5 and 15 Hz, and are normalized to a common level. First P and S arrivals (Pn, Sn) and Lg phase are indicated on the seismograms. Strong Lg phases are observed at stations with continental ray paths. Weak but clear Lg phases are observed at stations with ray paths across the East Sea.

of a_i, b_j, and Q_{ij}. Equation (8) is solved using the regularized least-squares QR factorization algorithm (LSQR method; Paige and Saunders, 1982). The damping parameter applied in this study is 0.01, which allows for a stable and fast inversion.

Analysis and Results

We calculated the equalized amplitudes ($\ln[A(f)/S(f)]$) of *Lg* by deconvolving the ground motions for source spectra. Figure 4 shows the equalized amplitudes at 1 Hz. The representative geometrical-spreading exponent term (γ) and the reference quality factor (Q_0^{mean}) were estimated from the equalized amplitudes by fitting a curve based on equation (6) under a least-squares sense. Here, parameters γ and Q_0^{mean} represent the representative path properties of the study area.

We chose seismograms with good signal-to-noise ratios. Also, every seismogram was examined manually. We excluded equalized amplitudes that outlie too much from the mean values for stable measurement of γ and Q_0^{mean}. Also, we did not include equalized amplitudes at distances less than 50 km, where *Lg* is not separated fully from the preceding major *S* phases. About 86% of equalized amplitudes were used for this study.

The geometrical-spreading exponent term was determined to be $\gamma = 0.75$, and the reference quality factor was estimated to be $Q_0^{\mathrm{mean}} = 498$. Here the estimated γ was greater than the typical value, which is given by 0.5 for *Lg* (Sereno *et al.*, 1988; Xie, 2002). In addition, the estimated Q_0^{mean} was smaller than that of central Asia, which is given by 591 (Xie, 2002). The high γ and low Q_0^{mean} suggest high attenuation with distance in the study region.

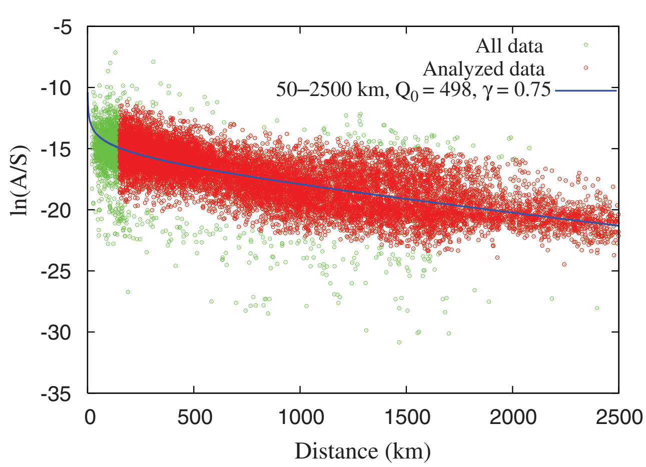

Figure 4. Variation of equalized *Lg* amplitudes, $\ln[A/S]$, with distance. Amplitude data that were significantly different from mean values were excluded for a stable inversion, which yielded 86% used (red dots) among the total data (red and green dots). The distances of data analyzed were 50–2500 km. The geometrical-spreading exponent term γ was estimated to be 0.75, and the mean quality factor at 1 Hz was determined to be 498. The inverted mean attenuation curve is presented with a solid line.

We performed an inversion based on equation (8) with implementation of the determined γ. The study area was discretized with 0.5°-by-0.5° cells. Inversion results are displayed for regions with cell-hit counts of 45 or more (see Fig. 1b).

To evaluate the resolution of the tomographic inversion, we performed two checkerboard tests. One model was composed of $2° \times 2°$ alternating positive and negative Q anomalies. The magnitudes of the Q perturbations are ± 249, which correspond to 50% of the mean quality factor (Fig. 5). In the other model, localized low Q regions were additionally included on the alternating-anomaly model. We considered realistic Q values in oceanic crust for the checkerboard test. We set the value of the localized low Q to be 40 (Fig. 6). We find that both the alternating perturbation patterns and the localized low Q perturbations are reasonably well resolved from the inversions (Figs. 5, 6).

Figure 7 shows the inverted LgQ_0. We observed high Q_0 anomalies in the western Korean Peninsula. In the Gyeongsang Basin region, the Cretaceous sedimentary basin in the southeastern part of the Korean Peninsula, we found low Q_0 anomalies. We also found high Q_0 in an eastern offshore region of the Korean Peninsula around the Hupo bank where a high gravity anomaly associated with magma underplating is observed (Cho *et al.*, 2004). In regions of the North Korea plateau, the South Korea plateau, and the Oki bank, we observed relatively high Q_0 compared to other oceanic regions. We also observed rapid transition of Q structure across the shores of the Korean Peninsula and Japanese islands.

We observed localized high Q_0 anomalies along the Japanese islands. Low Q_0 regions developed between the high Q_0 regions. The magnitude of the high Q_0 is comparable to that in the Korean Peninsula. The high Q_0 appears to reflect the property of the original continental lithosphere, which was separated from the Eurasian plate during the East Sea rifting period. Also, the low Q_0 in the Japanese islands appears to be associated with volcanic activity and mantle wedge convection over the subducting slabs of the Pacific and Philippine Sea plates.

It is intriguing to note that the *Lg* Q_0 variation is similar to the *Pn* velocity variation of Hong and Kang (2009). Note that *Pn* velocities are inverted from travel times, while *Lg* Q is inverted from wave amplitudes. The strong correlation between *Pn* velocities and *Lg* Q suggests that a structural variation in the crust and lithosphere produces coherent influence on both travel times and amplitudes of regional phases.

In most oceanic regions, including the East Sea (Sea of Japan), the East China Sea, and the Pacific Ocean, the *Lg* Q_0 is estimated to be significantly low ($Q_0 \leq 100$). The crust in the East Sea is a transitional structure between a continental crust and an oceanic crust. The observation of low Q_0 in most offshore regions suggests that *Lg* is significantly attenuated in oceanic regions. As a result, the magnitudes of oceanic events can be underestimated. Proper amplitude correction may be required for *Lg* waves that travel through oceanic regions.

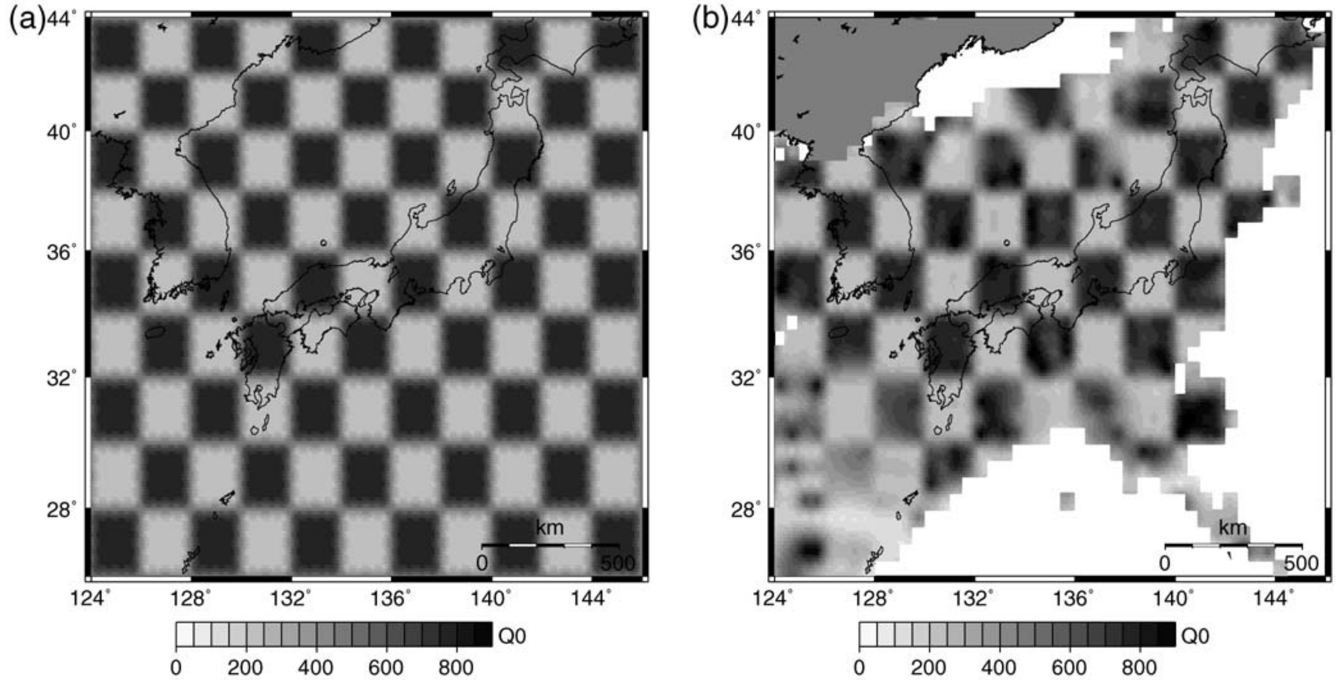

Figure 5. Checkerboard test for a medium with alternating positive and negative Q anomalies: (a) input model and (b) inverted Q tomographic image. The size of each anomaly is $2° \times 2°$. The values of the alternating Q anomalies are $Q_0^{\mathrm{mean}} \pm 249$. The tomographic inversion is conducted for a medium represented by cells with a size of 0.5°-by-0.5°. Tomographic inversion results for regions with cell-hit counts of 45 or more are presented. The input Q model is reasonably well recovered from the inversion.

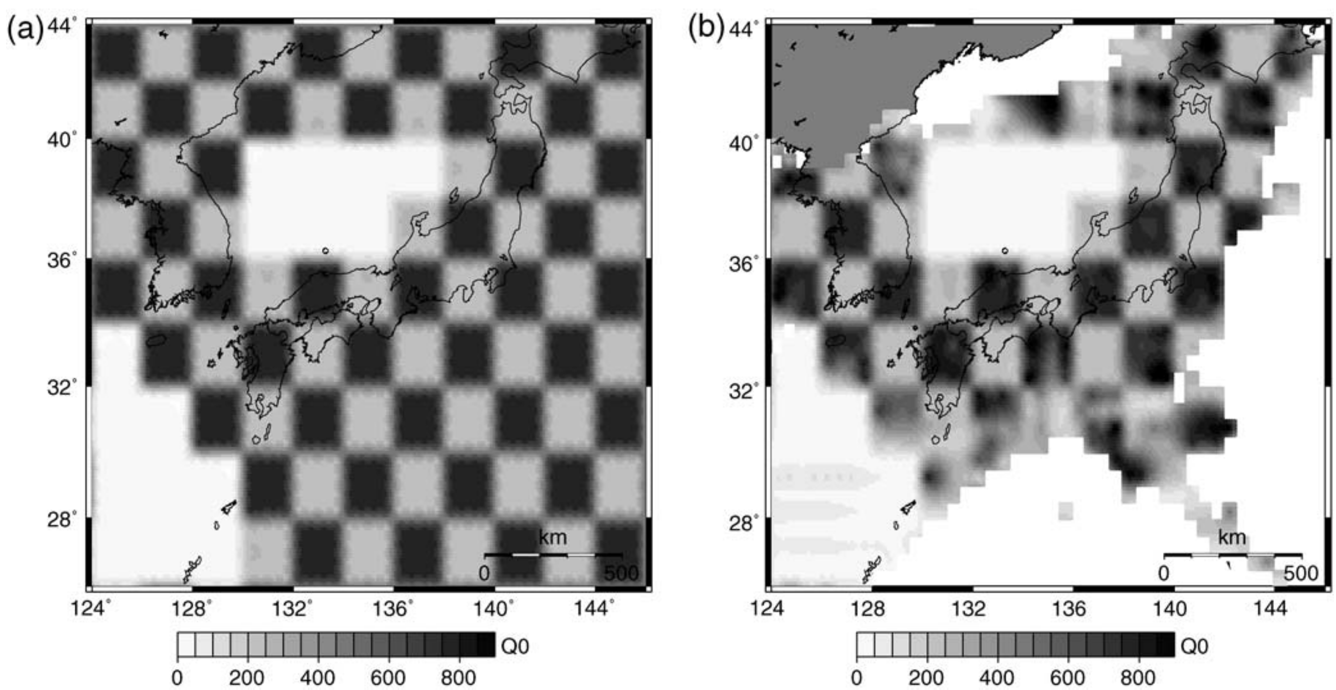

Figure 6. Checkerboard test for a medium with localized low Q blocks and alternating Q perturbations: (a) input model and (b) inverted Q tomographic image. The values of the alternating Q anomalies are $Q_0^{\mathrm{mean}} \pm 249$, and those of the localized low Q are 40. The medium is represented by cells with a size of 0.5°-by-0.5°. The tomographic inversion results are presented for regions with cell-hit counts of 45 or more. The input Q model is reasonably well recovered from the inversion.

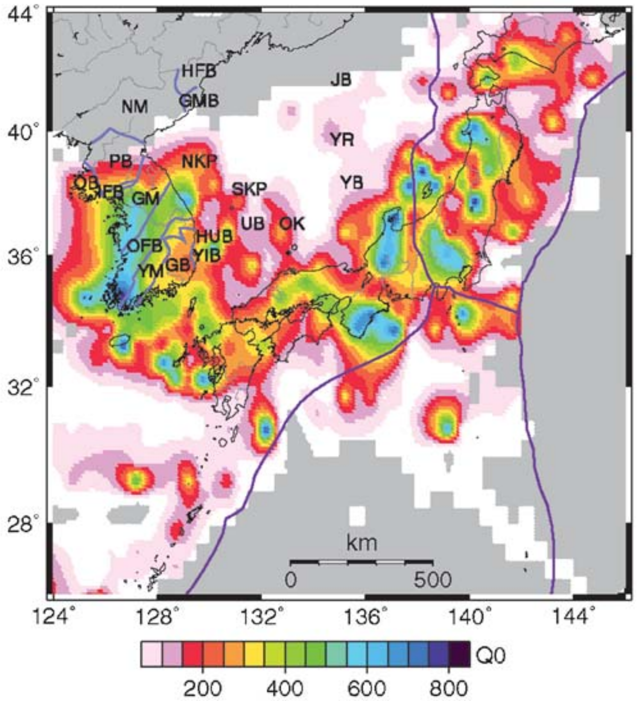

Figure 7. *Lg* Q_0 tomography. High Q_0 is observed in most regions of South Korea except the southeastern part where a volcanic-sediment basin develops. Japanese islands show patches of high Q_0 with intervening low Q structures. Significantly low Q_0 is observed in most oceanic regions. Plate boundaries and major tectonic structures are presented. GB, Gyeongsang Basin; GM, Gyeongsang massif; GMB, Gilju-Myeongcheon basin; HFB, Hambuk fold belt; HUB, Hupo bank and basin; IFB: Imjingang fold belt; JB, Japan basin; NKP, North-Korea plateau; NM, Nangnim massif; OB, Ongjin basin; OFB, Okcheon fold belt; OK, Oki bank; PB, Pyeongnam basin; SKP, South Korea plateau; UB, Ulleung basin; YB, Yamato basin; YIB, Yeonil basin; YM, Yeongnam massif; YR, Yamato rise.

Discussion and Conclusions

Lg is the largest phase typically recorded at regional distances. The *Lg* phase has often been used for estimation of magnitude of a regional event. It is well known that *Lg* is significantly influenced by lateral variation in crustal structure. However, the amount of *Lg* energy dissipated during propagation in oceanic regions has rarely been investigated. In this study, we investigated LgQ_0 variation in the continental margins around Korea and Japan, which are encompassed by sea and oceans.

The representative Q_0 value and the geometrical-spreading exponent term were estimated as 498 and 0.75 respectively, implying high attenuation compared to other intraplate regions. The quality factors in transitional crusts and oceanic environments are estimated to be less than 100. On the other hand, some areas in the Korean Peninsula and Japanese islands display high Q_0 values. The high Q_0 indicates the medium property of the original continental crust.

The low-Q region in the southeastern Korean Peninsula coincides with the Cretaceous volcanic-sediment region. Also, mixtures of high and low Q_0 along the Japanese islands are observed. The characteristic feature appears to be associated with volcanic activity and mantle-wedge convection. Many earthquakes occur in oceanic regions around Korea and Japan. Thus, it may be necessary to analyze the seismic amplitudes with proper correction of path-dependent attenuation for correct magnitude estimation.

Data and Resources

Seismic waveform data and earthquake information used in this study were collected from the web sites of the Korea Meteorological Administration (KMA, www.kma.go.kr, last accessed December 2008), the Korea Institute of Geoscience and Mineral Resources (KIGAM, quake.kigam.re.kr, last accessed December 2008), the Incorporated Research Institutions for Seismology (IRIS, www.iris.edu/data, last accessed December 2008), the National Research Institute for Earth Science and Disaster Prevention (NIED, www.fnet.bosai.go.jp, last accessed September 2008), and International Seismological Centre (ISC, www.isc.ac.uk, last accessed December 2008).

Some data were collected by visiting the institutes. Some figures were produced using Generic Mapping Tools (Wessel and Smith, 1998; gmt.soest.hawaii.edu, last accessed September 2008).

Acknowledgments

We are grateful to the Korea Meteorological Administration (KMA), the Korea Institute of Geoscience and Mineral Resources (KIGAM), the Incorporated Research Institutions for Seismology (IRIS), and the National Research Institute for Earth Science and Disaster Prevention (NIED) in Japan for making seismic data available. We thank Drs. Keith Koper, Sean Ford, and an anonymous reviewer for their constructive comments that improved the presentation of the paper. This work was supported by the program "Study on Development and Application of Earthquake Monitoring Techniques" of the National Institute of Meteorological Research and the Korea Meteorological Administration.

References

Aki, K., and P. G. Richards (1980). *Quantitative Seismology, Theory and Methods*, Vol. 1, W. H. Freeman and Company, San Franciso.

Brune, J. N. (1970). Tectonic stress and the spectra of seismic shear waves from earthquakes, *J. Geophys. Res.* **75,** no. 26, 4997–5009.

Campillo, M., J. L. Plantet, and L. Bouchon (1985). Frequency-dependent attenuation in the crust beneath central France from *Lg* waves: Data analysis and numerical modeling, *Bull. Seismol. Soc. Am.* **75,** 1395–1411.

Chang, S.-J., and C.-E. Baag (2005). Crustal structure in southern Korea from joint analysis of teleseismic receiver functions and surface-wave dispersion, *Bull. Seismol. Soc. Am.* **95,** 1516–1534.

Cho, H.-M., H.-J. Kim, H.-T. Jou, J.-K. Hong, and C.-E. Baag (2004). Transition from rifted continental to oceanic crust at the southeastern Korean margin in the East Sea (Japan Sea), *Geophys. Res. Lett.* **31,** L07606, doi 10.1029/2003GL019107.

Chough, S. K., S.-T. Kwon, J.-H. Ree, and D. K. Choi (2000). Tectonic and sedimentary evolution of the Korean peninsula: A review and new view, *Earth-Science Reviews* **52,** 175–235.

Chung, T. W., M.-H. Noh, J.-K. Kim, Y.-K. Park, H.-J. Yoo, and J. M. Lees (2007). A study of the regional variation of low-frequency Q_{Lg}^{-1} around the Korean Peninsula, *Bull. Seismol. Soc. Am.* **97,** 2190–2197.

Fisk, M. D. (2007). Corner frequency scaling of regional seismic phases for underground nuclear explosions at the Nevada Test Site, *Bull. Seismol. Soc. Am.* **97,** no. 3, 977–988.

Hearn, T. M., S. Wang, S. Pei, Z. Xu, J. F. Ni, and Y. Yu (2008). Seismic amplitude tomography for crustal attenuation beneath China, *Geophys. J. Int.* **174,** 223–234.

Hong, T.-K., and T.-S. Kang (2009). *Pn* travel-time tomography of the paleo-continental-collision and rifting zone around Korea and Japan, *Bull. Seismol. Soc. Am.* **99,** no. 1, 416–421.

Hong, T.-K., and J. Rhie (2009). Regional source scaling of the 9 October 2006 underground nuclear explosion in North Korea, *Bull. Seismol. Soc. Am.* **99,** no. 4, 2523–2540.

Hong, T.-K., C.-E. Baag, H. Choi, and D.-H. Sheen (2008). Regional seismic observations of the October 9, 2006 underground nuclear explosion in North Korea and the influence of crustal structure on regional phases, *J. Geophys. Res.* **113,** B03305, doi 10.1029/2007JB004950.

Jolivet, L., and P. Huchon (1989). Crustal scale strike-slip deformation in Hokkaido, Northeast Japan, *Struct. Geol.* **11,** 509–522.

Kennett, B. L. N. (1986). *Lg* waves and structural boundaries, *Bull. Seismol. Soc. Am.* **76,** 1133–1141.

Kennett, B. L. N., and T. Furumura (2001). Regional phases in continental and oceanic environments, *Geophys. J. Int.* **146,** no. 2, 562–568.

Kim, H.-J., H.-T. Jou, H.-M. Cho, H. Bijwaard, T. Sato, J.-K. Hong, H.-S. Yoo, and C.-E. Baag (2003). Crustal structure of the continental margin of Korea in the East Sea (Japan Sea) from deep seismic sounding data: Evidence for rifting affected by the hotter than normal mantle, *Tectonophysics* **364,** 25–42.

Knopoff, L., R. G. Mitchel, E. G. Kausel, and F. Schwab (1979). A search for the oceanic *Lg* phase, *Geophys. J. R. Astr. Soc.* **56,** 211–218.

Lay, T., and T. C. Wallace (1995). *Modern Global Seismology*, Academic Press, Inc., San Diego, California.

Paige, C. C., and M. A. Saunders (1982). LSQR: An algorithm for sparse linear equations and sparse linear systems, *ACM Trans. Math. Software* **8,** 195–209.

Phillips, W. S., H. E. Hartse, S. R. Taylor, and G. E. Randall (2000). 1 Hz *Lg Q* tomography in central Asia, *Geophys.. Res. Lett.* **174,** 223–234.

Sato, T., T. Sato, M. Shinohara, R. Hino, M. Nishino, and T. Kanazawa (2006). *P*-wave velocity structure of the margin of the southeastern Tsushima Basin in the Japan Sea using ocean bottom seismometers and airguns, *Tectonophysics* **412,** 159–171.

Sereno, T. J., Jr., S. R. Bratt, and T. C. Bache (1988). Simultaneous inversion of regional wave spectra for attenuation and seismic moment in Scandinavia, *J. Geophys. Res.* **93,** no. B3, 2019–2035.

Wessel, P., and W. H. F. Smith (1998). New, improved version of the Generic Mapping Tools released, *EOS Trans. AGU* **79,** 579.

Xie, J. (2002). Source scaling of *Pn* and *Lg* spectra and their ratios from explosions in central Asia: Implications for the identification of small seismic events at regional distances, *J. Geophys. Res.* **107,** no. B7, 2128, doi 10.1029/2001JB000509.

Xie, J., and H. J. Patton (1999). Regional phase excitation and propagation in the Lop or region of central Asia and implications for P/Lg discriminants, *J. Geophys. Res.* **104,** no. B1, 941–954.

Xie, J., Z. Wu, R. Liu, D. Schaff, Y. Liu, and J. Liang (2006). Tomographic regionalization of crustal *Lg Q* in eastern Eurasia, *Geophys. Res. Lett.* **33,** L03315, doi 10.1029/2005GL024410.

Zhang, T.-R., and T. Lay (1995). Why the *Lg* phase does not traverse oceanic crust, *Bull. Seismol. Soc. Am.* **85,** no. 6, 1665–1678.

Yonsei University
Department of Earth System Sciences
Shinchon-dong, 134, Seodaemun-gu
Seoul 120-749, South Korea
tkhong@yonsei.ac.kr

Manuscript received 25 February 2009